Korean J. Chem. Eng., 40(1), 145-154 (2023)
DOI: 10.1007/s11814-022-1188-y

pISSN: 0256-1115
eISSN: 1975-7220

Application of water scrubbing technique for biogas upgrading in a microchannel

Sara Behaien*, Babak Aghel*,†, and Mostafa Safdari Shadloo**

*Department of Chemical Engineering, Faculty of Energy, Kermanshah University of Technology, Kermanshah, Iran
**CORIA-CNRS (UMR 6614), Normandie University, INSA of Rouen, 76000 Rouen, France
(*Received 15 March 2022 • Revised 5 May 2022 • Accepted 26 May 2022*)

Abstract−Biogas, produced as a result of anaerobic degradation of organic matter, is an alternative source of renewable energy and a sustainable and cost-effective fuel due to its high availability. However, before it can be used as an energy source, biogas must be upgraded by removing impurities such as CO_2 and H_2S to increase its calorific value. In this study, CO_2 was removed and synthetic biogas was upgraded at atmospheric pressure in a microchannel using three absorbents of well water, seawater, and drinking water. The effects of operating variables, including absorbent flow rate, biogas flow rate, and system temperature, were investigated. As a function of independent variables, RSM analysis proposed a quadratic model for the absorption process by each absorbent to predict the response (CO_2 removal efficiency). Moreover, the experimental values obtained for CO_2 absorption were found to satisfactorily match the model values (R^2=0.9991-0.9997). The maximum CO_2 absorption in well water, seawater, and drinking water at 30 °C, liquid flow rate of 150 ml·h^{-1}, and gas flow rate of 50 ml·min^{-1} was 90.22, 84.95, and 79.66, respectively.

Keywords: Biogas Upgrading, Microchannel, Carbon Dioxide, Water Scrubbing, Seawater, Well Water

INTRODUCTION

Modern society is encountering a large volume of produced wastes and their treatment due to the construction and production of goods and services to meet social demands; but from another view, they find an opportunity to produce sustainable resources and energy through the development of circular economies. In developing countries, biogas can be produced by anaerobic digestion of wastes, especially agricultural waste, due to the abundance and availability of nutrients, resulting in the development of biomass energy, resource utilization, environment upgrading, and optimization of energy structure. Biogas can be used to replace traditional natural gas in automobile fuels, natural gas pipelines, chemical raw materials, combined heat and power units [1,2].

Raw biogas consists of 50-75% methane, 25-50% carbon dioxide, 0-10% nitrogen, 0-3% hydrogen sulfide, 0-1% hydrogen and other impurities [3]. The presence of undesired elements like CO_2, vapor, and H_2S, in the biogas diminishes its thermal value and can result in corrosion in gas pipelines, and increases the costs of compression and transportation [4]. The removal of these impurities, especially CO_2, is an important step in obtaining pure methane and upgrading raw biogas to a useable fuel. Pure biogas not only decreases the emission of greenhouse gases but also emits fewer hydrocarbons, nitrogen oxide, and carbon monoxide compared to gasoline and diesel. Modern technologies can remove most of these impurities and decrease considerably the thermal value of biogas [5,6].

Different technologies used to upgrade biogas include physical absorption (water scrubbing, organic physical scrubbing), chemical absorption, pressurized swing adsorption (PSA), vacuum swing adsorption (VSA), temperature swing adsorption (TSA), cryogenic technique, membrane separation, and biological technologies [7-11].

Chemical absorption by amine solution is a proven method for CO_2 removal with negligible loss of CH_4 and relatively low cost. However, the loss of absorbents (mainly ethanolamines) through degradation, evaporation, and high energy consumption to reduce the absorbent decreases the cost-effectiveness of the chemical absorption process [12-14].

Physical absorption like water or organic physical fluid absorbs the undesired elements of biogas [15]. Water scrubbing, which is the most widely used biogas upgrading technology throughout the world, uses the higher solubility of H_2S and CO_2 in water compared to CH_4 [16]. The solubility of CO_2 and CH_4 in water is 340 and 13.2 mmol·kg^{-1}, respectively, at 25 °C with gas at a partial pressure of 0.1 MPa [4,17]. CO_2 absorption in water is usually done by forming bicarbonate ions (HCO_3^-) at high pressure and low temperature to increase CO_2 solubility and allow selective CO_2 absorption from biogas [18].

Water scrubbing at high pressure is the most practical technology for biogas treatment due to its simplicity and reliability [19]. Benizri et al. [20] reported that using a scrubber increased biogas upgrading up to 77% at a pressure of 7.924 bar with an absorption efficiency of (57.5%) and a high methane recovery ratio (94%). However, according to Cozma et al. [15], the disadvantage is its higher electricity cost (0.34 kWh per cubic meter of raw biogas). Therefore, water scrubbing at near-atmospheric pressure has been proposed, which requires less specific electricity (0.24 kWh·m^{-3}) to upgrade raw biogas [21].

Geng et al. [22] and Walozi et al. [23] obtained the maximum purified CH_4 of 77 and 80%, respectively, using water scrubbing at atmospheric pressure.

For efficient transfer of CO_2 from biogas to liquid phase and up-

†To whom correspondence should be addressed.
E-mail: b.aghel@kut.ac.ir

grading of biogas in a multi-phase system, most units use spray towers, plate columns, and packed towers [24,25]. The disadvantages of these types of equipment are high volume, high energy consumption, high cost, difficult maintenance, low mass transfer coefficient, and low efficiency. Today, using microfluidic technology with exceptional properties of heat and mass transfer can use as a chemical reactor, excellent absorber, thermal exchanger, and mixer and has attracted the attention of researchers. The specific characteristic of a microreactor increases specific interfacial area and, as a result, it considerably intensifies mass transfer. To increase production capacity and high-power applications, microchannels can be used as parallel channels [26-29].

Akkarawatkhoosith et al. [30] obtained 98.9% purity methane in biogas upgrading at MEA-to-CO_2 molar ratio of 5 : 1, 50 °C, 3 bar, and 3 ml·min^{-1}. They found that the MEA to CO_2 molar ratio and temperature show a very strong effect and these parameters have an important interaction. Zhu et al. [31] studied CO_2 absorption by MEA solution in a T-junction microchannel and found that a high mass transfer coefficient can be obtained by increasing gas and liquid flow rate.

Since, seawater is rich in Ca^{2+} and Mg^{2+} ions and can directly increase the carbonate sediments to stabilize CO_2 and develop carbon capture and storage [32,33]. Various studies about the solubility of CO_2 in seawater have been carried out. Li and Tsui [34], using infrared gas analysis, determined CO_2 solubility in water, seawater, and NaCl solution. They found that CO_2 solubility in the seawater with NaCl solution in the same mass is similar. Li et al. [35] used artificial seawater in cell equilibrium to absorb CO_2 and reported that by increasing the pressure and reducing the temperature and salinity, CO_2 absorption increases.

This study, by using inexpensive absorbents, tried to solve the economic problem of biogas upgrading. Since seawater is not available in some areas and well water and drinking water contain Ca^{2+} and Mg^{2+} ions and have smaller amounts of salt than seawater, well water and drinking water as absorbents were used and compared. Using different sources of water CO_2 absorption was investigated in a microchannel at atmospheric pressure, within a temperature range of 10-50 °C, and with different liquid and gas flow rates.

Table 1. Characteristics and composition of absorbents

Measured quantity	Drinking water	Well water	Seawater
pH	7.37	7.5	8.05
TDS	110	377.7	44,082
TH	47	274.3	-
Ca^{2+}	11.5	70.7	478
Mg^{2+}	4.3	23.6	1,268
Na^{+}	16.7	6.9	7,906
K^{+}	-	-	543
Nitrate	2.3	-	-
Nitrite	0.05>	-	-
Fluoride	0.05	-	-
SO_4^{2-}	21.4	24.2	2,466
Cl^{-}	-	14.3	20,855
CO_3^{2-}	-	0	154
HCO_3^{-}	-	295.9	-
Br^{-}	-	-	72
S^{2-}	-	-	822
Ni^{2+}	-	-	0.324

All of the concentrations are in ppm (mg/L)

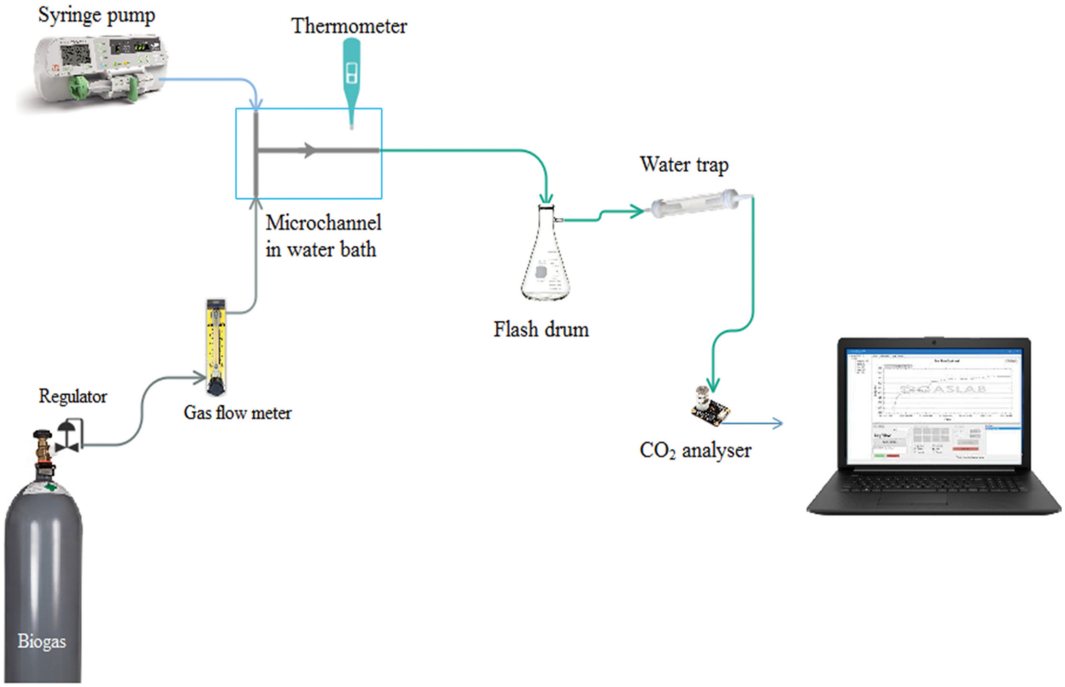

Fig. 1. Schematic of the biogas upgrading process.

Table 2. Range and level of variables

Factor	Name	Units	Level				
			$-\alpha$	−1	0	+1	$+\alpha$
A	Temperature	°C	10	20	30	40	50
B	Gas flow rate	$ml \cdot min^{-1}$	50	100	150	200	250
C	Liquid flow rate	$ml \cdot h^{-1}$	50	100	150	200	250

MATERIALS AND METHODS

The absorbents used in this study included seawater (Persian Gulf water), well water, and drinking water. Biogas is a mixture of 60% CH_4 and 40% CO_2 obtained from Aryan Gas Company. Table 1 presents the absorbent compositions used in this study.

1. Experimental Setup and Procedure

Fig. 1 depicts the devices used for the biogas upgrading process. The absorption process took place in a T-shaped stainless steel microchannel with a channel length of 25 cm and a circular cross-section with an inner diameter of 800 μm. The intensive mixing process is performed in a T-shaped micromixer to create a high level of contact between the two phases. To adjust the system temperature, the microchannel was placed in a water bath and its temperature was controlled using a thermometer with an accuracy of ±1 °C. The microchannel had two inflows: the first inflow was biogas, which was adjusted using an LZB-WB flowmeter, with an accuracy of 5% at a flow rate of 50-250 $ml \cdot min^{-1}$. The second flow contained the absorbent (seawater, well water, and drinking water) that was pumped into the microchannel using a syringe pump from Sondes Teb Company within an injection range of 0.1-1,200 $ml \cdot h^{-1}$. At the junction, both the gas and liquid flows were mixed and CO_2 was absorbed through the microchannel. The microchannel outflow entered a 250 ml vacuum Erlenmeyer flask to separate the gas and liquid flows.

The liquid remained in the lower part of the vacuum Erlenmeyer flask and the upgraded biogas left through the upper opening of the flask, then passed through the water trap to remove the remaining moisture.

The gas composition was monitored with a CO_2 sensor (SprintIR®- W100) every second, and the amount of CO_2 was calculated as follows:

$$CO_2 \text{ removal } (\%) = \frac{CO_{2\,in} - CO_{2\,out}}{CO_{2\,in}} \times 100 \quad (1)$$

2. Experimental Design and Statistical Analysis

CO_2 absorption efficiency in continuous systems is determined by the temperature, absorbent flow rate, and gas flow rate. Therefore, an experimental design based on the central composite approach to obtain the best acceptable solution under controllable experimental conditions was used. Based on the literature [18,30, 31,36] the proper ranges of temperature, gas flow rate, and liquid flow rate with were selected for the experiments.

The central composite design (CCD) method is a response surface method and all independent parameters were considered on five different levels ($+\alpha$, +1, 0, −1, $-\alpha$) in the course of the analysis, suggesting a set of 20 runs (with six repetitions of the central point). Table 2 presents a list of factors and levels in this study.

Since a quadratic model is commonly used to model real-life processes [37], a polynomial quadratic model is also used here to predict CO_2 absorption efficiency, as a function of the independent inputs, in proportion to the empirical data obtained through the multiple regression analysis to estimate the values of the model coefficients (Eq. (2)).

$$Y = b_0 + \Sigma_{i=1}^{k} b_i x_i + \Sigma_{i=1}^{k} b_{ii} x_i^2 + \Sigma_{i=1}^{k} \Sigma_{j>1}^{k} b_{ij} x_i x_j + \varepsilon \quad (2)$$

where Y is the response variable, x_i is the dimensionless coded input variable for X_i, b is the regression constant, i and j are index numbers, ε denotes the random error, and k represents the number of the factors that are studied and optimized. Afterward, the analysis of variance (ANOVA) method was used in the regression analysis to estimate the regression equation coefficient and evaluate the quality and significance of the model.

RESULTS AND DISCUSSION

1. CO_2 Solubility Reactions

As shown in Fig. 2, the dissolution behavior of CO_2 in water is divided into three phases: CO_2 is transferred from the gas phase to the liquid phase. As CO_2 enters the liquid phase, the first separation takes place, and HCO_3^- and H^+ are produced (Eq. (3)). In the second separation process, CO_3^{2-} and H^+ are produced (Eq. (4)).

Afterward, CO_3^{2-}, Ca^{2+}, and Mg^{2+} in the solution form the $CaCO_3$ and $MgCO_3$ sediments (Eqs. (5) and (6)).

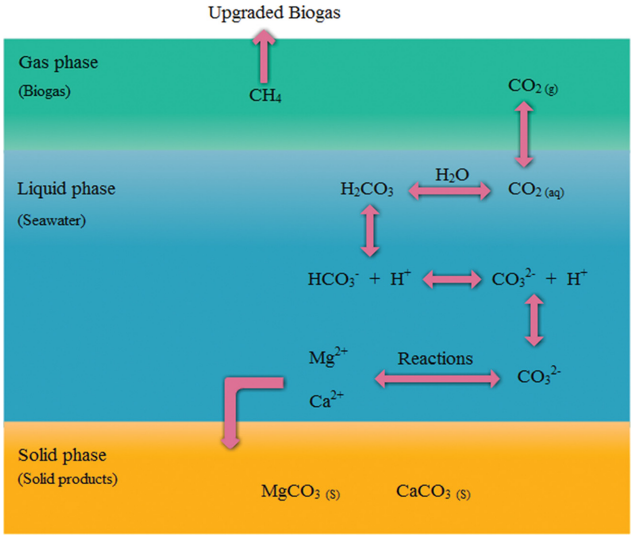

Fig. 2. Biogas upgrading and CO_2 solubility in seawater.

Table 3. Designing experiments using the CCD method and response

Run	A: Temp (°C)	B: Q_g ($ml \cdot min^{-1}$)	C: Q_l ($ml \cdot h^{-1}$)	Response CO_2 removal efficiency (%)		
				Well water	Seawater	Drinking water
1	10	150	150	61.55	65.55	62.35
2	20	200	200	48.98	62.35	49.58
3	30	150	250	60.23	68.65	65.35
4	30	150	150	57.32	52.91	60.55
5	30	150	150	56.03	52.25	60.65
6	30	150	150	56.98	52.98	60.95
7	20	100	100	70.32	66.21	69.68
8	30	250	150	35.55	47.55	28.95
9	30	150	150	56.65	51.55	60.18
10	30	150	50	50.32	43.21	49.48
11	50	150	150	35.55	50.02	46.35
12	40	100	100	58.55	60.03	58.55
13	40	200	200	35.35	52.32	43.26
14	20	100	200	83.65	74.56	77.98
15	30	150	150	57.01	51.98	59.85
16	30	150	150	56.55	52.03	60.12
17	30	50	150	90.22	84.95	79.66
18	20	200	100	46.325	46.32	45.6
19	40	100	200	66.32	68.55	71.25
20	40	200	100	38.58	35.59	37.18

Table 4. Final equations in terms of coded factors

CO_2 removal efficiency	Correlation
Well water	$56.78-6.40A-13.68B+2.52C+0.9656AB-1.43AC-2.71BC-2.04A^2+1.55B^2-0.3574C^2$
Seawater	$52.32-4.00A-9.22B+6.28C-1.07AB+0.1088AC+1.99BC+1.39A^2+3.51B^2+0.9280C^2$
Drinking water	$60.39-4.04A-12.70B+3.92C+0.3900AB+0.8125AC-1.37BC-1.51A^2-1.52B^2-0.7401C^2$

$$CO_2\,(l)+H_2O \leftrightarrow HCO_3^- + H^+ \quad (3)$$

$$HCO_3^- \leftrightarrow CO_3^{2-} + H^+ \quad (4)$$

$$Ca^{2+}+CO_3^{2-} \leftrightarrow CaCO_3 \quad (5)$$

$$Mg^{2+}+CO_3^{2-} \leftrightarrow MgCO_3 \quad (6)$$

2. Design of Experiment and Statistical Analysis Method

RSM was used to analyze the effect of parameters on the absorption efficiency of CO_2. The effects of independent variables, namely temperature (A), gas flow rate (B), and liquid flow rate (C), on the response were determined through experiments. These experiments for each absorbent (seawater, well water, and drinking water) included 20 tests as listed in Table 3.

RSM proposes a quadratic model for the biogas upgrading process by all three absorbents based on the independent variables (equations in Table 4). The value and sign of each coefficient in this relation indicate the effects of reducing and increasing the response parameters. The coded equations are useful for identifying the relative effect of the parameters by comparing the coefficients of the factors. For example, in the relation proposed for CO_2 removal efficiency in seawater, the relative importance of the independent factors is as follows: A (temperature), B (gas flow rate), and C (liquid flow rate) coefficient values obtained for the model were −4.00, −9.29, and 6.28, respectively. The maximum interaction between parameters coefficient is +1.99, which is related to the B and C.

Table 5 presents the ANOVA and statistical parameters for CO_2 removal efficiency in the well water, seawater, and drinking water liquids. If the experimental data shows significant regression and the lack of fit is insignificant, the model fits properly. The value of the calculated probability (P-value) is an important parameter for determining the significance of the terms in each model. P-values lower than 0.05 also show the significance of the model terms. Based on the ANOVA results presented in Table 5, the proposed models are statistically significant due to the low P-value, which is less than 0.0001.

The coefficient of determination (R^2) values obtained for well water, seawater, and drinking water are 0.9997, 0.9991, and 0.9995, respectively. These values demonstrate the fit and adequacy of the regression model. The high R^2 value shows the good fit between the actual and the calculated results within a wide range of experiments as shown in Table 6.

Table 5. ANOVA of response surface quadratic model (A) well water, (B) seawater, and (C) drinking water

(A)

Source	Sum of squares	df	Mean square	F-value	p-Value	
Model	4,046.67	9	449.63	3,468.27	<0.0001	Significant
A-T	656.32	1	656.32	5,062.60	<0.0001	
B-Qg	2,996.06	1	2,996.06	23,110.42	<0.0001	
C-Ql	101.73	1	101.73	784.72	<0.0001	
AB	7.46	1	7.46	57.54	<0.0001	
AC	16.37	1	16.37	126.30	<0.0001	
BC	58.73	1	58.73	452.99	<0.0001	
A^2	104.50	1	104.50	806.08	<0.0001	
B^2	60.02	1	60.02	462.98	<0.0001	
C^2	3.21	1	3.21	24.78	0.0006	
Residual	1.30	10	0.1296			
Lack of fit	0.2829	5	0.0566	0.2791	0.9062	Not significant
Pure error	1.01	5	0.2027			
Cor total	4,047.97	19				

(B)

Source	Sum of squares	df	Mean Square	F-value	p-value	
Model	2,609.67	9	289.96	1,246.19	<0.0001	Significant
A-T	256.08	1	256.08	1,100.57	<0.0001	
B-Qg	1,361.06	1	1,361.06	5,849.50	<0.0001	
C-Ql	631.39	1	631.39	2,713.57	<0.0001	
AB	9.18	1	9.18	39.46	<0.0001	
AC	0.0946	1	0.0946	0.4066	0.5380	
BC	31.56	1	31.56	135.64	<0.0001	
A^2	48.70	1	48.70	209.29	<0.0001	
B^2	309.40	1	309.40	1,329.74	<0.0001	
C^2	21.65	1	21.65	93.05	<0.0001	
Residual	2.33	10	0.2327			
Lack of fit	0.7537	5	0.1507	0.4791	0.7808	Not significant
Pure error	1.57	5	0.3146			
Cor total	2,612.00	19				

(C)

Source	Sum of squares	df	Mean square	F-value	p-Value	
Model	3,206.77	9	356.31	2,312.40	<0.0001	Significant
A-Temp	260.82	1	260.82	1,692.71	<0.0001	
B-Q G	2,582.16	1	2,582.16	16,757.98	<0.0001	
C-Q L	246.49	1	246.49	1,599.69	<0.0001	
AB	1.22	1	1.22	7.90	0.0185	
AC	5.28	1	5.28	34.27	0.0002	
BC	14.96	1	14.96	97.09	<0.0001	
A^2	57.05	1	57.05	370.26	<0.0001	
B^2	57.91	1	57.91	375.82	<0.0001	
C^2	13.77	1	13.77	89.38	<0.0001	
Residual	1.54	10	0.1541			
Lack of fit	0.7257	5	0.1451	0.8903	0.5492	Not significant
Pure error	0.8151	5	0.1630			
Cor total	3,208.31	19				

Adequate precision calculates the signal-to-noise ratio by comparing the range of the predicted values at the design points with the average prediction error. The adequate precision values obtained for well water, seawater, and drinking water were 216.5801, 144.6039, and 183.0736, respectively. These values proved that the model had adequate signals. The coefficient of variance values for well water,

Table 6. Fit statistics

	Well water	Seawater	Drinking water
R^2	0.9997	0.9991	0.9995
Adjusted R^2	0.9994	0.9983	0.9991
Predicted R^2	0.9991	0.9968	0.9981
Adequate precision	216.5801	144.6039	183.0736
Standard deviation (SD)	0.3601	0.4824	0.3925
Mean	56.10	56.98	57.38
Coefficient of variance (CV%)	0.6418	0.8466	0.6841

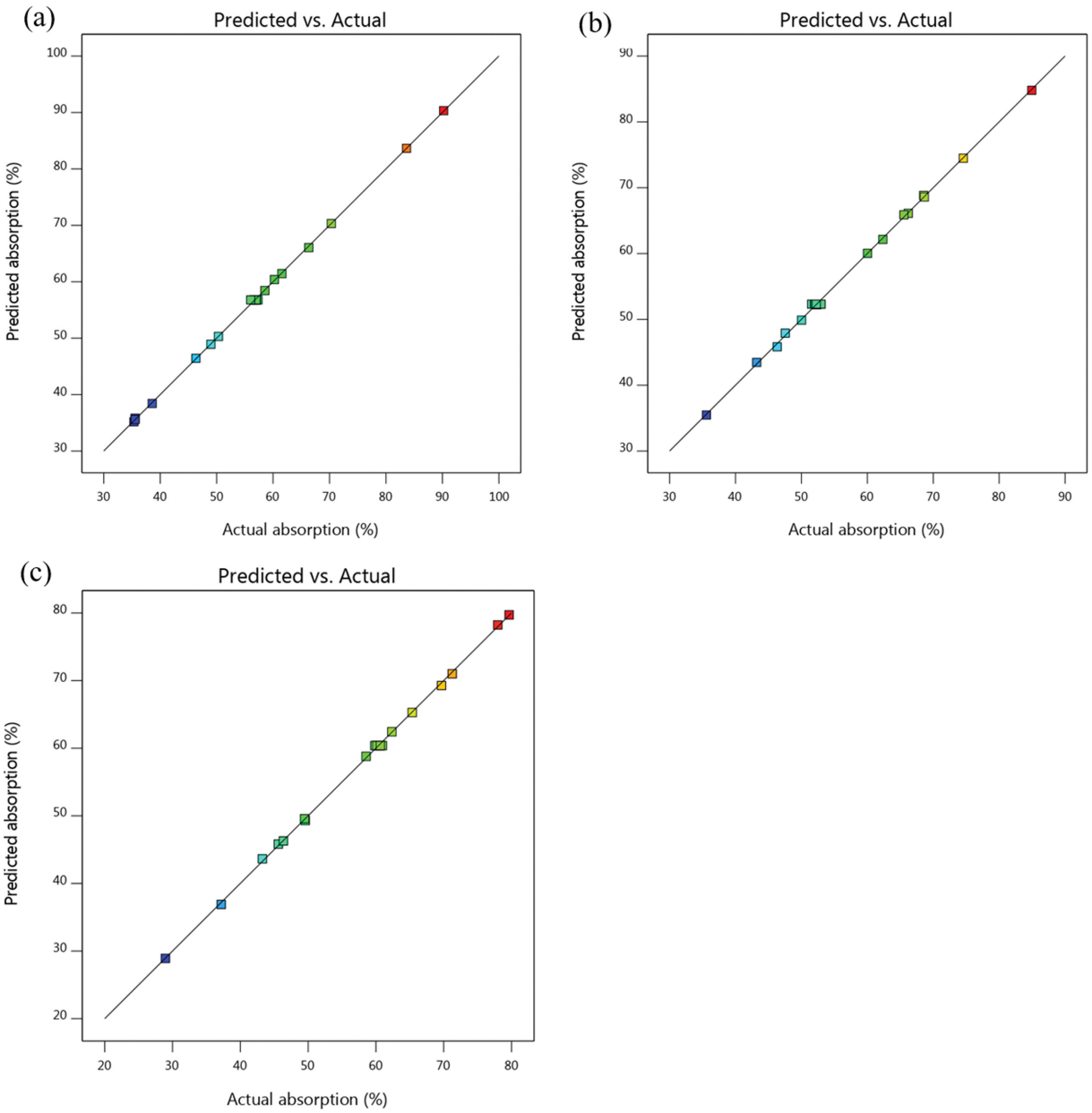

Fig. 3. The CCD predicted value of CO_2 removal efficiency vs. actual absorption with (a) groundwater (b) seawater (c) drinking water.

seawater, and drinking water were 0.6418, 0.8466, and 0.6841%, respectively. These values indicated the reproducibility of the created model.

The diagram of the actual values versus the predicted values of CO_2 removal efficiency is shown in Fig. 3. Based on this diagram, the residuals are on a straight line, the predicted outputs are highly

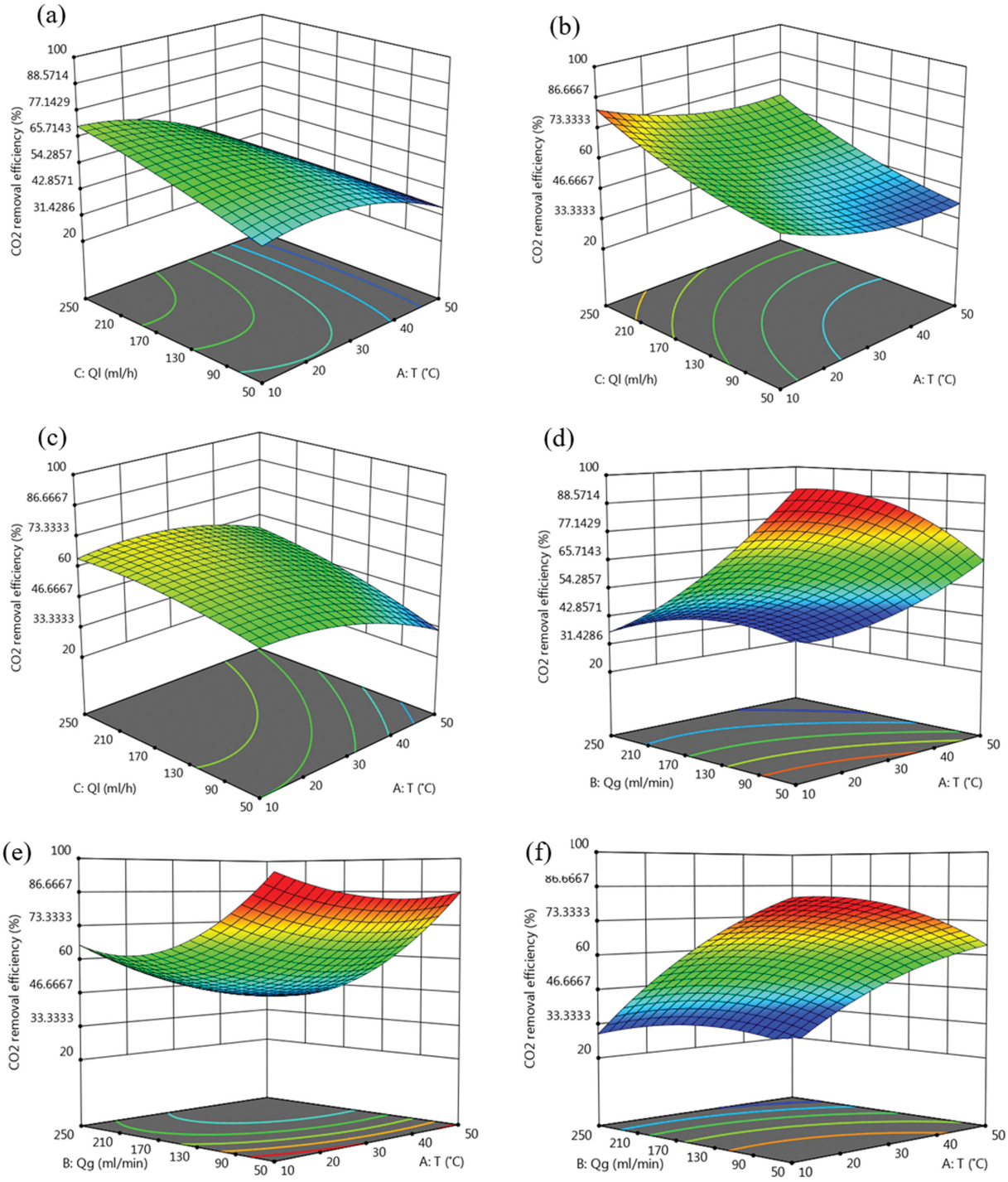

Fig. 4. Response surfaces plots of CO_2 removal efficiency of (a) liquid flow rate and temperature (well water), (b) liquid flow rate and temperature (seawater), (c) liquid flow rate and temperature (drinking water), (d) gas flow rate and temperature (well water), (e) gas flow rate and temperature (seawater), (f) gas flow rate and temperature (drinking water), (g) liquid flow rate and gas flow rate (well water), (h) liquid flow rate and gas flow rate (seawater), (i) liquid flow rate and gas flow rate (drinking water).

correlated with the observed outputs, and they show a good signal for the regression model.

3. Interactive Effects of Process Parameters

Three-dimensional graphical representations are in Fig. 4 to evaluate the effects of various independent variables on CO_2 absorption or biogas upgrading. As seen in Fig. 4(a)-(c), with a decrease in temperature and an increase in the liquid flow rate, the CO_2 removal efficiency increases for all three liquid absorbents. As the temperature rises, Henry's constant increases, and a smaller amount of CO_2 is dissolved in water [38-40]. As seen in Fig. 4(a)-(c), the purity of biogas increases with the liquid flow rate because, with an increase in the amount of the solvent and the contact between the liquid

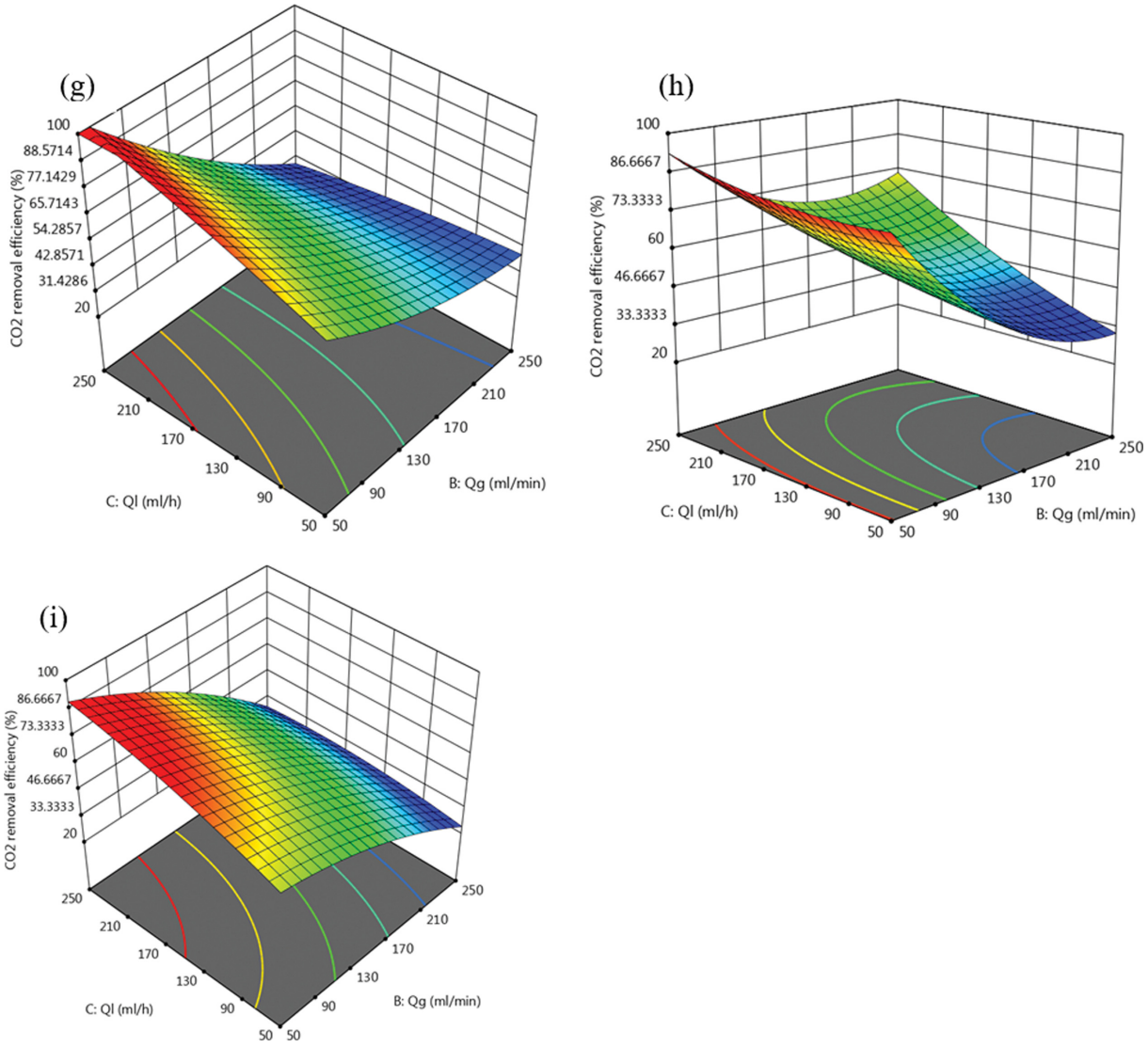

Fig. 4. Continued.

and biogas, more CO_2 is removed from biogas [3,41]. Hence, the low temperature and high flow rate of the liquid increase the biogas upgrading.

The biogas flow rate had the greatest effect on the biogas upgrading (Fig. 4(d)-(i)). As the biogas flow rate increases, CO_2 removal decreases drastically (Fig. 4(d)-(i)) [3,20,39,40], and because the Q_g/Q_l ratio rises substantially, the movement of bubbles in the microchannel is accelerated, and there is no adequate contact between CO_2 and the water molecules. As a result, the duration of interaction between the gas and liquid phases decreases. At a certain liquid flow rate, more CO_2 is placed along the microchannel as the gas flow rate increases, causing a decrease in the liquid phase absorption capacity with a higher gas flow rate [40,42].

When the Q_g/Q_l ratio is at the lowest level, the highest CO_2 removal rate is obtained in all absorbents. When the gas flow rate is at the lowest level, the highest CO_2 removal is 90.22%, 84.95%, and 79.66% in well water, seawater, and drinking water, respectively. Considering the high rate of mass transfer in the microchannel compared to other mass transfer devices on the macro scale [30], more CO_2 transfers from the gas to the liquid phase, and biogas is upgraded through physical absorption.

As seen in Table 7, the Q_g/Q_l ratios in this study were considerably lower than the Q_g/Q_l in common devices ratio to upgrade biogas. Therefore, much less equipment is needed to supply temperature and pressure. In addition, the size of the devices used in this work is much smaller than traditional equipment and requires less space. No chemical additives are required to adjust the pH of the system.

In summary, well water was the best absorbent for the biogas upgrading process. Since well water and seawater have a higher pH than drinking water, they were better absorbents for CO_2. Furthermore, due to the large amount of salt and unwanted Cl^{-1} ions in seawater, this absorbent had lower absorption efficiency than well water. Although, seawater can be suggested as the best absorbent due to its low cost and availability. Moreover, $CaCO_3$ and $MgCO_3$ sediments are formed with the absorption of CO_2, which

Table 7. Comparison of different biogas upgrading absorption systems

Absorber	Absorbent	Inlet gas	Q_g	Q_l	Temperature	Pressure	CO_2 removal (%)	Ref.
Absorption tower	Water	45% CO_2 and air	400 ($L \cdot h^{-1}$)	200 ($L \cdot h^{-1}$)	17.0-20.0 °C	1.2 MPa	94.2	[38]
Packed column	Water+ NaHCO3	60% CH_4 40% CO_2	14.1 ($ml \cdot min^{-1}$)	21.15 ($ml \cdot min^{-1}$)	20 °C	Atmospheric	91.3 CH_4 content	[3]
Packed scrubber with bottom column	Water	55% CH_4 45% CO_2	40.7 ($Nm^3 \cdot h^{-1}$)	8.243 ($m^3 \cdot h^{-1}$)	12 °C	7.924 bar	57.5	[20]
Absorption column	water	CH_4/CO_2 ratio: 0.96	4850.2 ($L \cdot h^{-1} \cdot m^2$)	3100.3 ($L \cdot h^{-1} \cdot m^2$)	9.05 °C	1 bar	70	[39]
Packed column	water	Raw biogas	1.75 ($m^3 \cdot h^{-1}$)	2 ($m^3 \cdot h^{-1}$)	-	10 bar	92.67	[41]
Microchannel	Well water	60% CH_4 40% CO_2	50 ($ml \cdot min^{-1}$)	150 ($ml \cdot h^{-1}$)	30 °C	Atmospheric	90.22	This study
Microchannel	Seawater	60% CH_4 40% CO_2	50 ($ml \cdot min^{-1}$)	150 ($ml \cdot h^{-1}$)	30 °C	Atmospheric	84.95	This study
Microchannel	Drinking water	60% CH_4 40% CO_2	50 ($ml \cdot min^{-1}$)	150 ($ml \cdot h^{-1}$)	30 °C	Atmospheric	79.66	This study

Table 8. CO_2 absorption optimization by CCD

	A: T (°C)	B: Q_g ($ml \cdot min^{-1}$)	C: Q_l ($ml \cdot h^{-1}$)	CO_2 absorption
Well water	31.12	53.33	229.53	99.25
Seawater	11.87	50.83	184.75	94.33
Drinking water	17.53	50.04	212.97	89.320

have numerous applications, due to the large number of Ca^{2+} and Mg^{2+} ions.

According to Henry's law, an increase in pressure increases the solubility of CO_2 and many processes of physical absorption with water have been performed at pressures higher than the atmospheric pressure to improve biogas improvement in the previous research [16,20,43]. However, in this study, given the use of intense mixing, the high contact surface and the high mass transfer coefficient of the microchannel, a high level of biogas purity at atmospheric pressure was obtained.

4. Optimization

The RSM optimization proposed various combinations of variables for obtaining the maximum absorption efficiency based on the experiments conducted. In this study, the input data values for the range values were entered to obtain the maximum CO_2 removal rate. Therefore, the optimal points for the highest CO_2 removal rate from biogas were 99.25, 94.33, and 89.32 for well water, seawater, and drinking water, respectively (Table 8).

CONCLUSION

Well water, seawater, and drinking water were used to separate CO_2 from biogas in a T-shaped microchannel at atmospheric pressure. The effects of important operating parameters, including temperature, gas flow intensity, and liquid flow intensity, were examined. RSM was used to develop a suitable model with the least-squares method. The experimental values obtained for CO_2 absorption were found to satisfactorily match the model values, and the R^2 values for well water, seawater, and drinking water were 0.9997, 0.9991, and 0.9995, respectively. The CO_2 absorption efficiency can be increased by increasing the liquid flow rate as well as decreasing the gas flow rate and temperature. The maximum CO_2 absorption in well water, seawater, and drinking water at 30 °C, liquid flow rate of 150 $ml \cdot h^{-1}$, and gas flow rate of 50 $ml \cdot min^{-1}$ was 90.22, 84.95, and 79.66, respectively. Note that the absorbent consumption is very low compared to previous studies due to the high Q_g/Q_l ratio. Seawater and well water have high absorption due to the abundance of Ca^{2+} and Mg^{2+} ions. By RSM optimization, the maximum CO_2 removal efficiency using well water of 99.25% was at 31.12 °C, a gas flow rate of 53.33 $ml \cdot min^{-1}$, and a liquid flow rate of 229.53 $ml \cdot h^{-1}$. According to the results, it can be argued that biogas upgrading in a microchannel using physical absorption at atmospheric pressure with seawater is low-cost, safe, and very cost-effective compared to chemical absorbents. Therefore, the use of this absorption and the construction of a biogas upgrading plant based on microchannel in coastal areas and areas with abundant well water has a high potential.

REFERENCES

1. H. M. Morgan Jr., W. Xie, J. Liang, H. Mao, H. Lei, R. Ruan and Q. Bu, *Bioresour. Technol.*, **250**, 910 (2018).
2. D. Li, M. Kim, H. Kim, O. Choi, B. I. Sang, P. C. Chiang and H. Kim, *Korean J. Chem. Eng.*, **35**(1), 179 (2018).
3. R. Noorain, T. Kindaichi, N. Ozaki, Y. Aoi and A. Ohashi, *J. Cleaner Prod.*, **214**, 103 (2019).
4. F. R. Abdeen, M. Mel, M. S. Jami, S. I. Ihsan and A. F. Ismail, *Chin. J. Chem. Eng.*, **24**(6), 693 (2016).
5. Q. Zhao, E. Leonhardt, C. MacConnell, C. Frear and S. Chen, *Compressed Biomethane, CSANR, Ed*, 24 (2010).
6. B. Aghel, S. Behaein, S. Wongwises and M. S. Shadloo, *Biomass*

Bioenergy, **160**, 106422 (2022).
7. O. W. Awe, Y. Zhao, A. Nzihou, D. P. Minh and N. Lyczko, *Waste Biomass Valorization*, **8**(2), 267 (2017).
8. B. Aghel, M. Maleki, S. Sahraie and E. Heidaryan, *Fuel*, **306**, 121636 (2021).
9. P. van Vu, V. C. Nguyen and J. Kim, *Korean J. Chem. Eng.*, **38**(8), 1676 (2021).
10. F. Jin, H. Xu, D. Hua, L. Chen, Y. Li, Y. Zhao and B. Zuo, *Korean J. Chem. Eng.*, **38**(1), 129 (2021).
11. G. Chen, F. Wang, S. Wang, C. Ji, W. Wang, J. Dong and F. Gao, *Korean J. Chem. Eng.*, **38**(1), 46 (2021).
12. I. Angelidaki, L. Treu, P. Tsapekos, G. Luo, S. Campanaro, H. Wenzel and P. G. Kougias, *Biotechnol. Adv.*, **36**(2), 452 (2018).
13. B. Aghel, S. Sahraie and E. Heidaryan, *Energy*, 117618 (2020).
14. B. Aghel, S. Sahraie, E. Heidaryan and K. Varmira, *Process Saf. Environ. Protection*, **131**, 152 (2019).
15. P. Cozma, C. Ghinea, I. Mămăligă, W. Wukovits, A. Friedl and M. Gavrilescu, *Clean - Soil, Air, Water*, **41**(9), 917 (2013).
16. R. Kapoor, P. M. V. Subbarao, V. K. Vijay, G. Shah, S. Sahota, D. Singh and M. Verma, *Appl. Energy*, **208**, 1379 (2017).
17. D. Deublein and A. Steinhauser, *Biogas from waste and renewable resources*, John Wiley & Sons, Weinheim, Germany (2008).
18. Y. Xiao, H. Yuan, Y. Pang, S. Chen, B. Zhu, D. Zou, J. Ma, L. Yu and X. Li, *Chin. J. Chem. Eng.*, **22**(8), 950 (2014).
19. K. Ghaib and F.-Z. Ben-Fares, *Renew. Sustain. Energy Rev.*, **81**, 433 (2018).
20. D. Benizri, N. Dietrich, P. Labeyrie and G. Hébrard, *Sep. Purif. Technol.*, **219**, 169 (2019).
21. W. M. Budzianowski, C. E. Wylock and P. A. Marciniak, *Energy Convers. Manage.*, **141**, 2 (2017).
22. H. Geng, Q. Chen and G. Zhao, The Experiment Study of Biogas Atomization Upgrading with Water Scrubbing at Atmospheric Pressure, in *2015 International Conference on Industrial Technology and Management Science*, 293 (2015).
23. R. Walozi, B. Nabuuma and A. Sebiti, *Univers. J. Agric. Res.*, **4**, 60 (2016).
24. Y. Tamhankar, B. King, J. Whiteley, T. Cai, K. McCarley, M. Resetarits and C. Aichele, *Chem. Eng. Res. Des.*, **104**, 376 (2015).
25. H. Salimi, N. Hashemipour, J. Karimi-Sabet and Y. Amini, *Chem. Prod. Process Model.* (2021).
26. B. Aghel, E. Heidaryan, S. Sahraie and S. Mir, *J. Cleaner Prod.*, **231**, 723 (2019).
27. P. Abdollahi, J. Karimi-Sabet, M. A. Moosavian and Y. Amini, *Sep. Purif. Technol.*, **231**, 115875 (2020).
28. P. F. Jahromi, J. Karimi-Sabet, Y. Amini and H. Fadaei, *Chem. Eng. J.*, **328**, 1075 (2017).
29. P. F. Jahromi, J. Karimi-Sabet and Y. Amini, *Chem. Eng. J.*, **334**, 2603 (2018).
30. N. Akkarawatkhoosith, A. Kaewchada and A. Jaree, *J. Taiwan Inst. Chem. Eng.*, **98**, 113 (2019).
31. C. Zhu, C. Li, X. Gao, Y. Ma and D. Liu, *Int. J. Heat Mass Transfer.*, **73**, 492 (2014).
32. A. Dastbaz, J. Karimi-Sabet, H. Ahadi and Y. Amini, *Desalination*, **424**, 62 (2017).
33. H. Li, Z. Tang, X. Xing, D. Guo, L. Cui and X. zhong Mao, *Energy*, **164**, 1135 (2018).
34. Y. Li and T. Tsui, *J. Geophys. Res.*, **76**, 4203 (1971).
35. C. Li, C. Zhu, Y. Ma, D. Liu and X. Gao, *Int. J. Heat Mass Transfer.*, **78**, 1055 (2014).
36. A. Asfaram, M. Ghaedi, M. H. A. Azqhandi, A. Goudarzi and M. Dastkhoon, *RSC Adv.*, **6**, 40502 (2016).
37. Y. Xiao, H. Yuan, Y. Pang, S. Chen, B. Zhu, D. Zou, J. Ma, L. Yu and X. Li, *Chin. J. Chem. Eng.*, **22**(8), 950 (2014).
38. C. Pirola, F. Galli, C. L. Bianchi and F. Manenti, *Technology*, **3**, 99 (2015).
39. B. Aghel, A. Gouran and S. Behaein, *Chem. Eng. Process. Process Intensif.*, **175**, 108927 (2022).
40. M. M. C. Rajivgandhi and M. Singaravelu, *Environ. Biotechnol.*, **7**(3), 639 (2014).
41. A. L. Kohl and R. Nielsen, *Gas purification*, Elsevier (1997).
42. J. Läntelä, S. Rasi, J. Lehtinen and J. Rintala, *Appl. Energy*, **92**, 307 (2012).